

2D Layer Arrangement of Solely [HS-HS] or [LS-LS] Molecules in the [HS-LS] State of A Dinuclear Fe(II) Spin Crossover Complex

Fabian Fürmeyer, Luca M. Carrella and Eva Rentschler *

Department of Chemistry, Johannes Gutenberg University Mainz, Duesbergweg 10–14, 55128 Mainz,
Germany; fuermeyer@uni-mainz.de (F.F.); carrella@uni-mainz.de (L.M.C.)

* Correspondence: rentschler@uni-mainz.de

Table of content

NMR spectra	
¹ H- and ¹³ C-NMR of I ⁴ MTD	p. 3
Mass spectrum of I ⁴ MTD	p. 4
IR spectra of dried C1 – C3	p. 4
X-ray diffraction measurements	
Molecular structure of C1 at 173 K	p. 6
Crystal packing of C1 at 173 K	p. 6
Molecular structure of C2 at 173 K	p. 7
Crystal packing of C2 at 173 K	p. 7
Molecular structure of C3 at 100 and 200 K	p. 8
Crystallographic parameters for all structures of C1 and C2	p. 8
Magnetic data	
C1 and C2	p. 9
C3 at different time periods	p. 9

NMR Spectroscopy

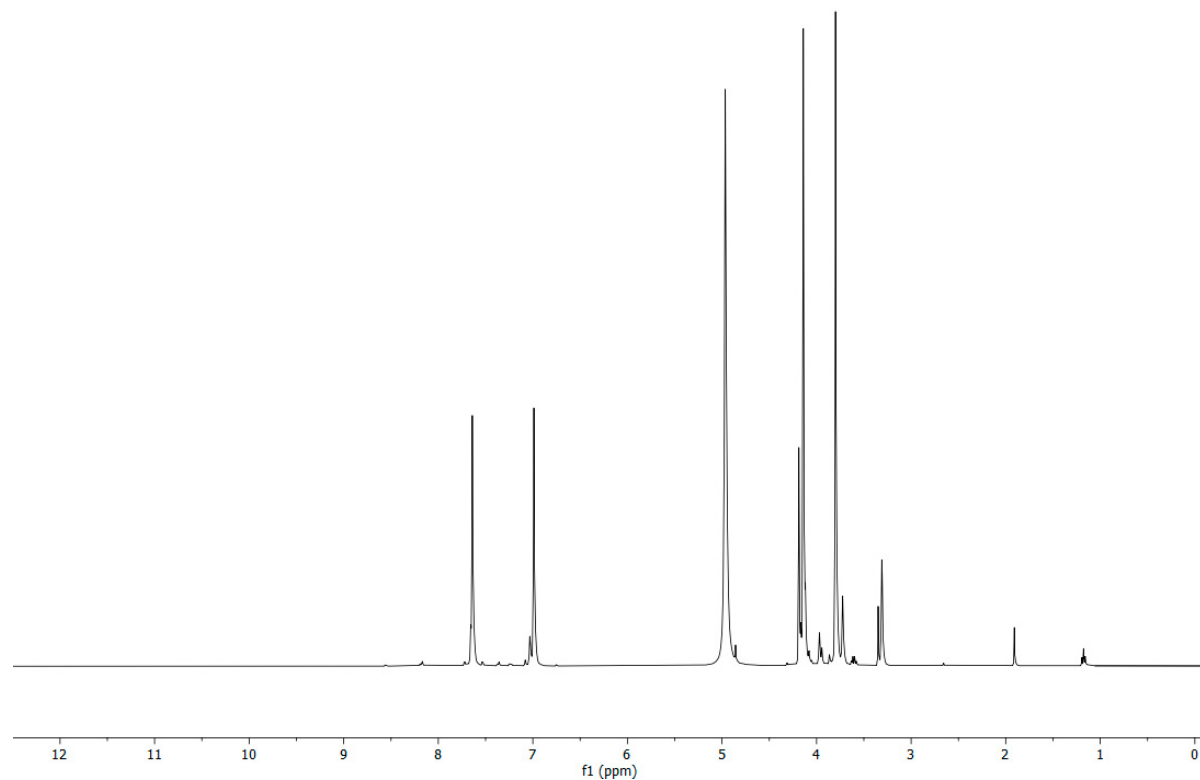


Figure S1. ¹H-NMR of 2,5-bis{[(1*H*-imidazol-4-ylmethyl)amino]methyl}-1,3,4-thiadiazole (**I⁴MTD**).

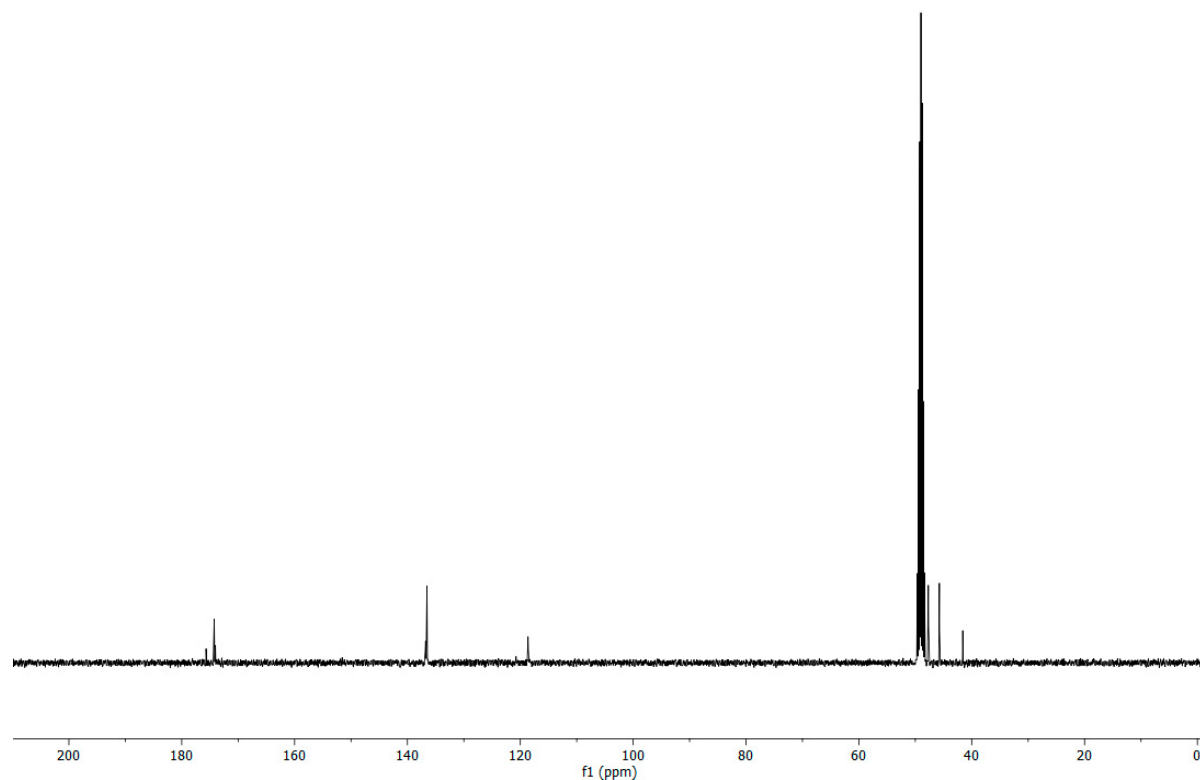


Figure S2. ¹³C-NMR of 2,5-bis{[(1*H*-imidazol-4-ylmethyl)amino]methyl}-1,3,4-thiadiazole (**I⁴MTD**).

Mass Spectrometry

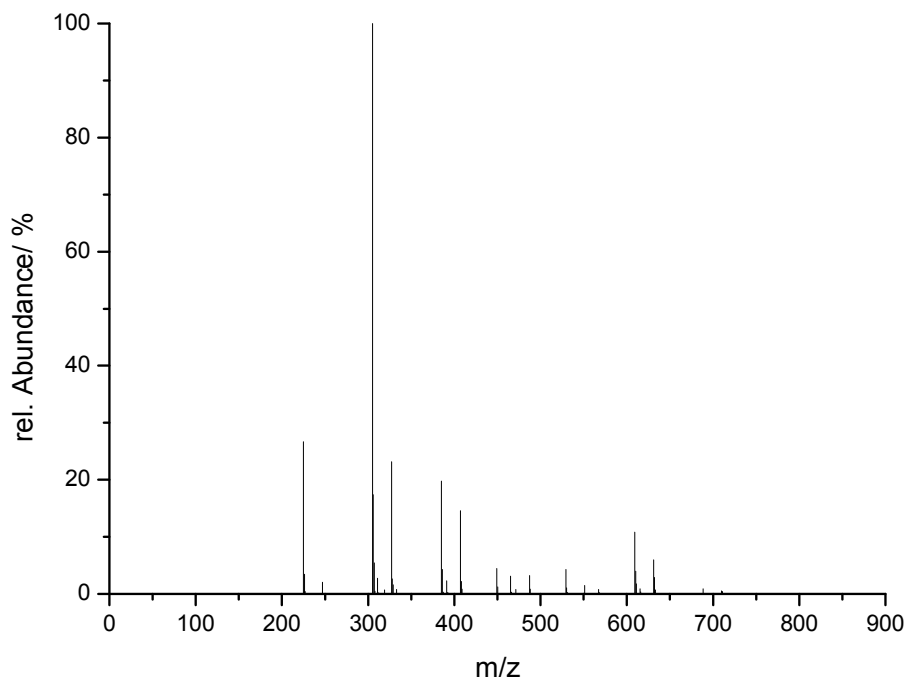


Figure S3. Field desorption mass spectrum of 2,5-bis{[(1*H*-imidazol-4-ylmethyl)amino]methyl}-1,3,4-thiadiazole (**I⁴MTD**).

IR Spectroscopy

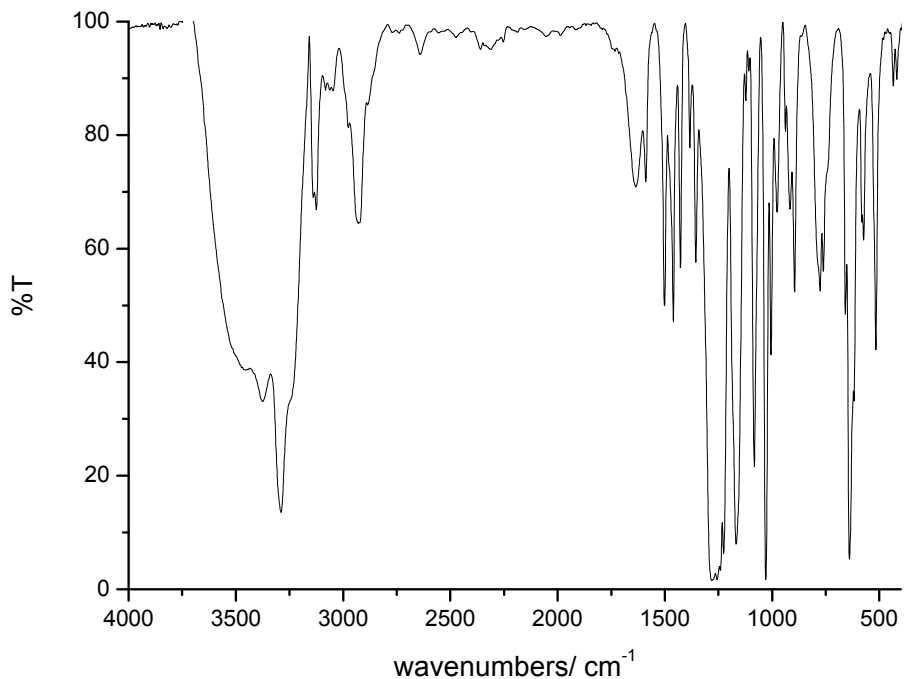


Figure S4. IR spectrum of air-dried $[\text{Fe}^{II}]_2(\text{I}^4\text{MTD})_2](\text{F}_3\text{CSO}_3)_4$ (**C1**).

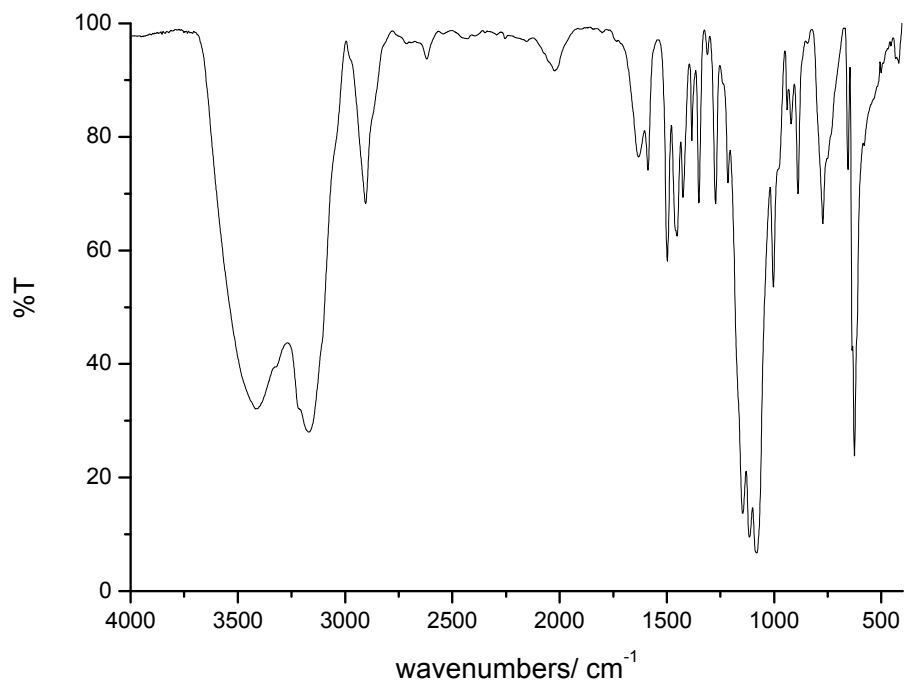


Figure S5. IR spectrum of air-dried $[\text{Fe}^{\text{II}}_2(\text{I}^4\text{MTD})_2](\text{ClO}_4)_4$ (**C2**).

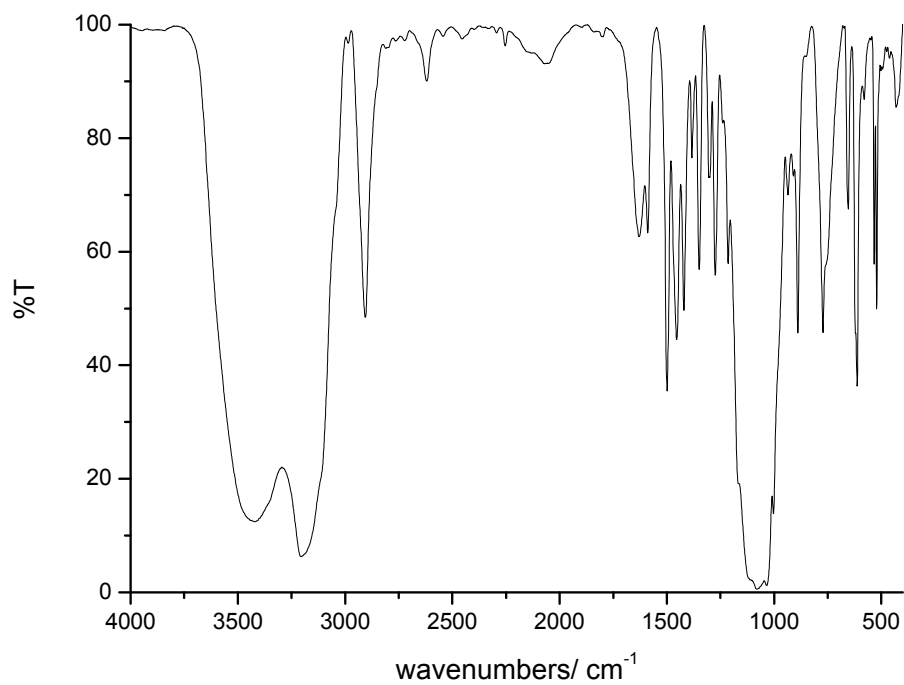


Figure S6. IR spectrum of air-dried $[\text{Fe}^{\text{II}}_2(\text{I}^4\text{MTD})_2](\text{BF}_4)_4$ (**C3**).

X-ray Diffraction Measurements

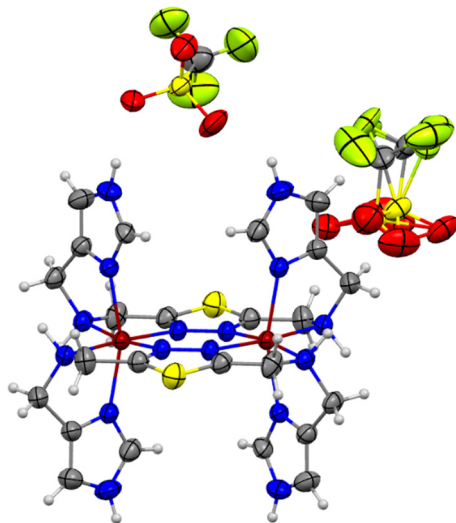


Figure S7. Molecular structure of $[\text{Fe}^{\text{II}}_2(\text{I}^4\text{MTD})_2](\text{F}_3\text{CSO}_3)_4*\text{solvents}$ ($\text{C}1*\text{solvents}$) with thermal ellipsoids at 173 K. Solvent molecules could not be solved. Color code: Fe is dark red, N blue, S yellow, C grey, H white, O red and F light green.

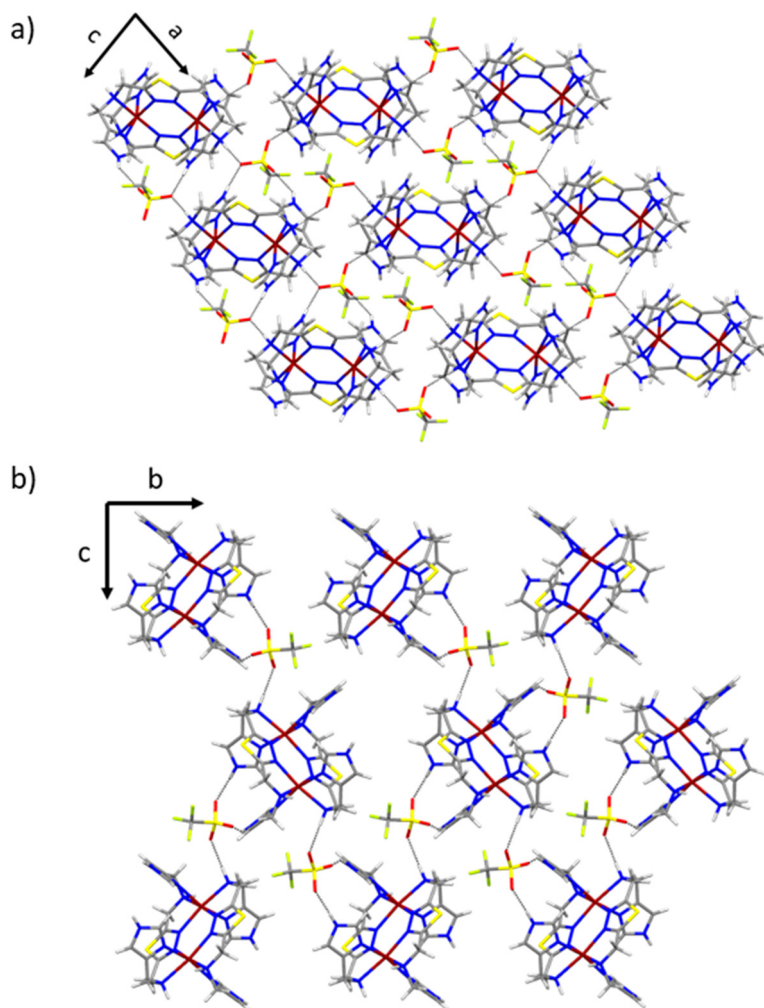


Figure S8. Crystal packing and hydrogen bonding (black dashed lines) via anions in $[\text{Fe}^{\text{II}}_2(\text{I}^4\text{MTD})_2](\text{F}_3\text{CSO}_3)_4*\text{solvents}$ ($\text{C}1*\text{solvents}$) at 173 K. Non-bridging counter ions have been omitted for clarity. **a)** View along crystallographic *b*-axis. **b)** View along crystallographic *a*-axis. Color code: Fe is dark red, N blue, S yellow, C grey, H white, O red and F light green.

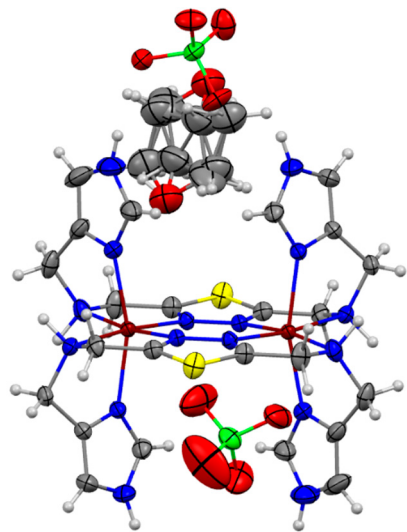


Figure S9. Molecular structure of $[\text{Fe}^{\text{II}}_2(\text{I}^4\text{MTD})_2](\text{ClO}_4)_4 \cdot \text{THF}$ (**C2*THF**) with thermal ellipsoids at 173 K. Color code: Fe is dark red, N blue, S yellow, C grey, H white, O red and Cl green.

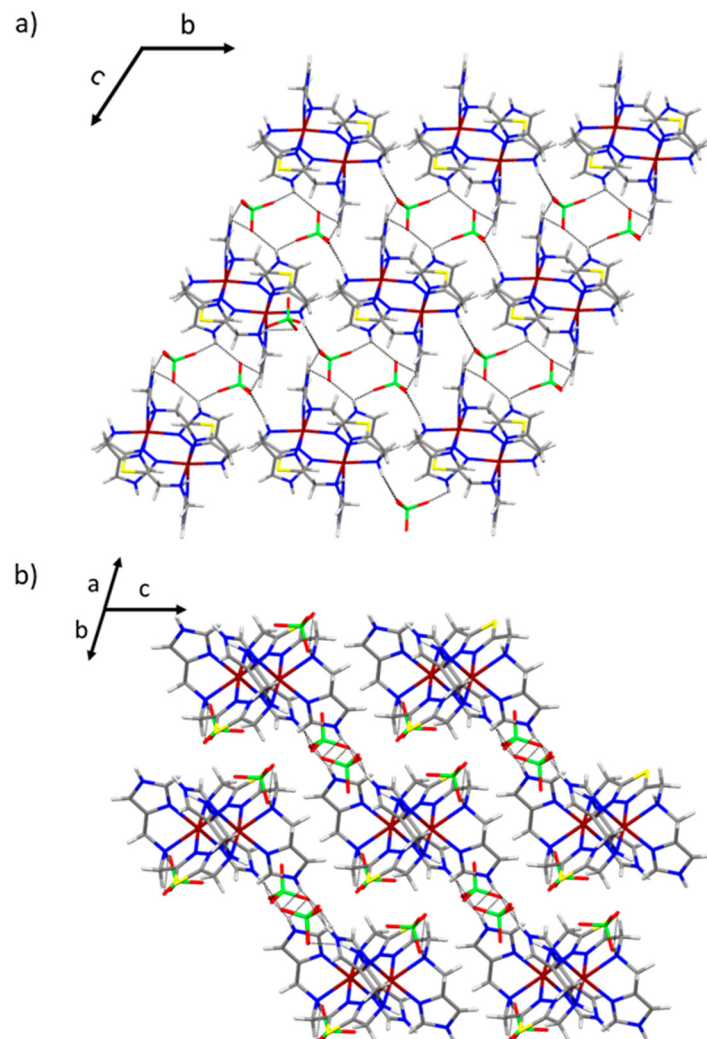


Figure S10. Crystal packing and hydrogen bonding (black dashed lines) via anions in $[\text{Fe}^{\text{II}}_2(\text{I}^4\text{MTD})_2](\text{ClO}_4)_4 \cdot \text{THF}$ (**C2*THF**) at 173 K. Non-bridging counter ions and solvent molecules have been omitted for clarity. **a)** View along crystallographic *a*-axis. **b)** View along the angle bisector of the crystallographic *a*- and *b*-axis. Color code: Fe is dark red, N blue, S yellow, C grey, H white, O red and Cl green.

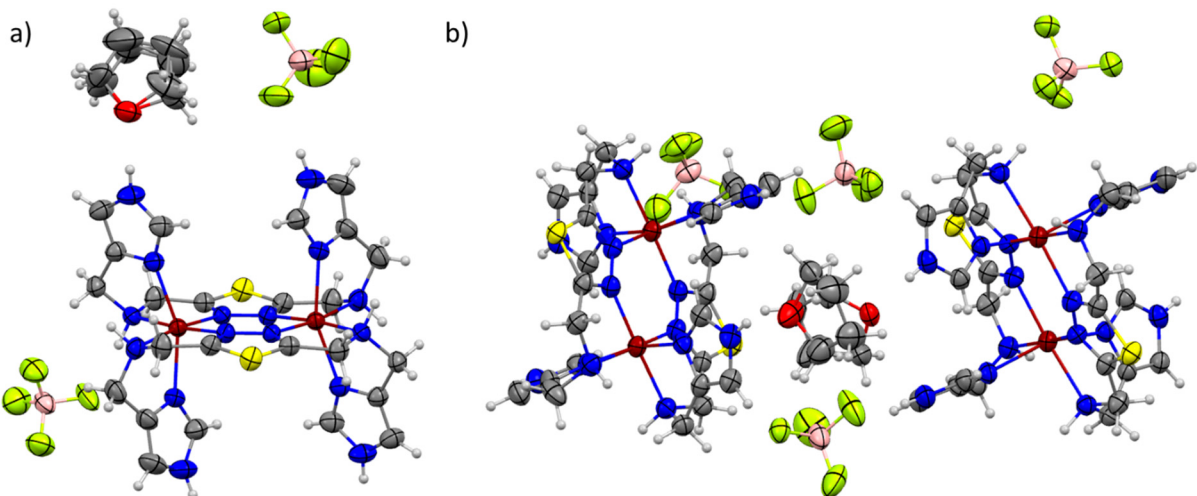


Figure S11. Molecular structure of $[\text{Fe}^{\text{II}}_2(\text{I}^4\text{MTD})_2](\text{BF}_4)_4\text{*THF}(\text{C}3\text{*THF})$ with thermal ellipsoids at **a)** 200 K and **b)** 100 K. Color code: Fe is dark red, N blue, S yellow, C grey, H white, O red, B pink and F light green.

Table S1. Crystallographic parameters for all discussed crystal structures of **C1 – C3**.

	C1*solvents (@173 K)	C2*THF (@173 K)	C3*THF (@100 K)	C3*THF (@200 K)
formula	C28 H32 F12 Fe2 N16 O12 S6	C28 H40 Cl4 Fe2 N16 O17 S2	C64 H96 B8 F32 Fe4 N32 O4 S4	C128 H192 B16 F64 Fe8 N64 O8 S8
molar weight [g/mol]	1316.75	1190.38	2423.84	4847.68
crystal system	monoclinic	triclinic	monoclinic	orthorombic
space group	C2/c	P-1	P2 ₁ /c	Pbca
a/ \AA	19.7359(6)	10.3301(9)	23.2819(9)	19.1991(3)
b/ \AA	12.3918(2)	11.0779(10)	18.9278(6)	10.6968(2)
c/ \AA	23.0394(7)	11.5540(9)	10.8273(4)	24.2411(5)
$\alpha/\text{^\circ}$	90	116.252(6)	90	90
$\beta/\text{^\circ}$	110.176(2)	90.726(7)	93.334(3)	90
$\gamma/\text{^\circ}$	90	107.913(7)	90	90
V/ \AA^3	5288.8(3)	1111.07(18)	4763.2(3)	4978.37(16)
Z	4	1	2	1
T/K	173(2)	173(2)	100(2)	200(2)
$\rho_{\text{calcd.}} [\text{g/cm}^3]$	1.654	1.779	1.69	1.617
$\mu [\text{mm}^{-1}]$	0.895	1.077	0.812	0.777
R(int)	0.0313	0.0177	0.0488	0.0317
S	1.058	1.057	1.053	1.082
R1 ($I > 2\sigma(I)$)	0.0511	0.0455	0.1316	0.0432
wR2 (all data)	0.1438	0.124	0.3981	0.1402

Magnetic data

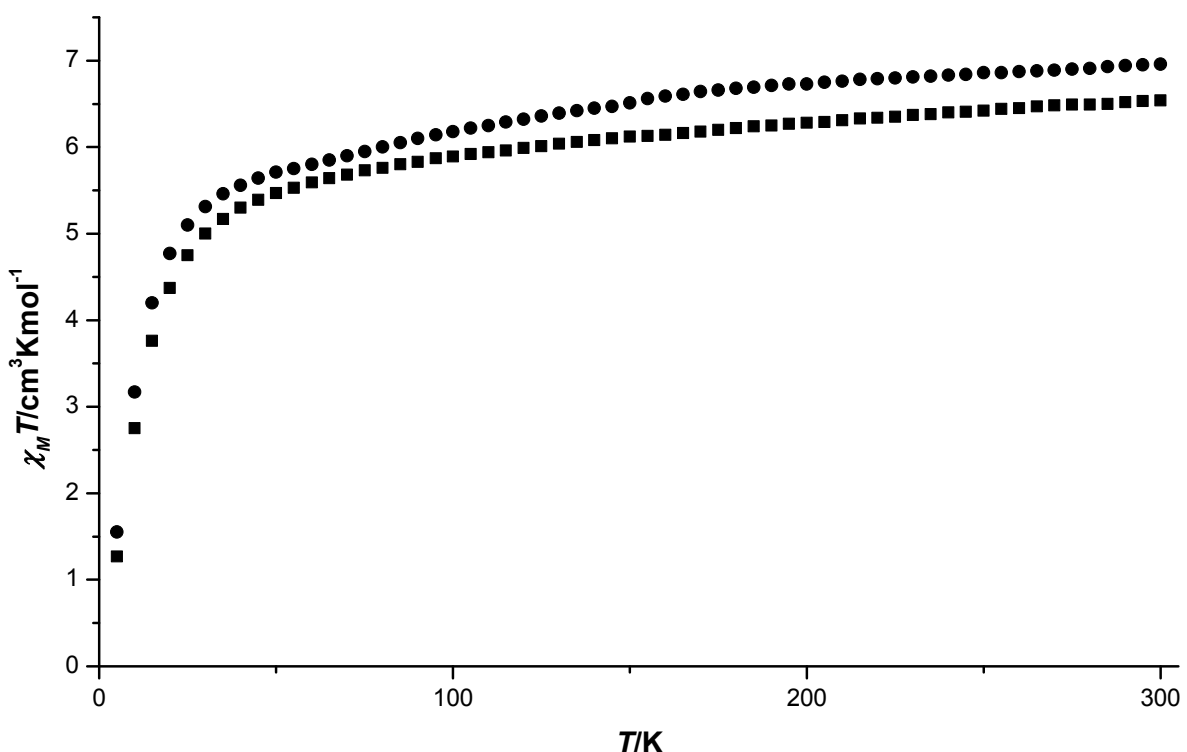


Figure S12. $\chi_M T$ vs T data for the air-dried compounds **C1** (squares) and **C2** (triangles). The data are given per dinuclear iron(II) molecule.

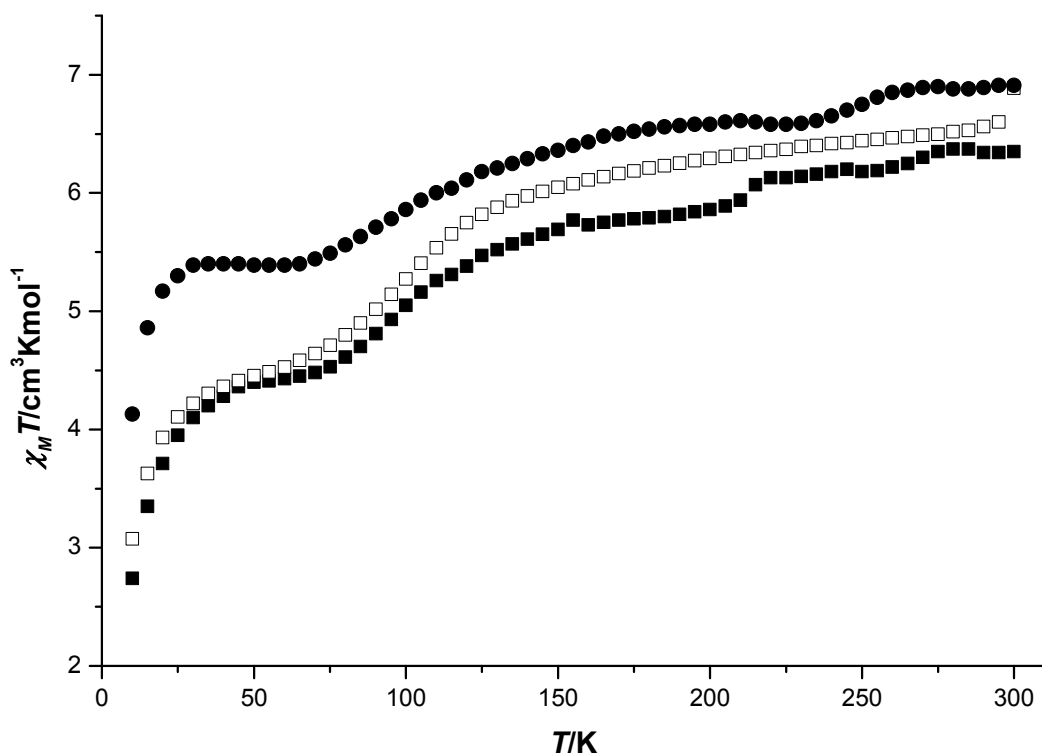


Figure S13. $\chi_M T$ vs T data for **C3** for a freshly taken sample measured from 10 – 300 K after direct low-temperature freezing within the magnetometer (filled squares), subsequently measured from 300 - 10 K (empty squares) and for a dried sample from 10 – 300 K after heating the sample to 400 K for 2 hours (filled circles). The data are given per dinuclear iron(II) molecule.